Stem Cell Reports, Volume *2*

Supplemental Information

Genetic and Chemical Correction of Cholesterol Accumulation and Impaired Autophagy in Hepatic and Neural Cells Derived from Niemann-Pick Type C Patient-Specific iPS Cells

Dorothea Maetzel, Sovan Sarkar, Haoyi Wang, Lina Abi-Mosleh, Ping Xu, Albert W. Cheng, Qing Gao, Maisam Mitalipova, and Rudolf Jaenisch

Inventory of Supplemental Information

Supplementary Figures

Figure S1: Generation and Characterization of NPC Patient-Specific iPSCs,

Related to Figure 1

Figure S2: Correction of *NPC1*I1062T Mutation in Patient-Specific iPSCs, Related

to Figure 2

Figure S3: Analysis of Cholesterol Metabolism in isogenic NPC1 iPSC-Derived

Cells, Related to Figure 3

Figure S4: Genetic Correction of Autophagy Phenotype in NPC1 iPSC-derived

cells, Related to Figure 4

Figure S5: Chemical Correction of Autophagy Phenotype in NPC1 iPSC-derived

cells, Related to Figure 5

Table S1: Summary of TALEN-mediated Genome Editing, Related to Figure 2

Supplementary Methods

Describing details of methodologies used

Supplementary References

References related to Supplementary Methods

Supplementary Note

Describing statistical analyses (p values) of Main Figures

Figure S1

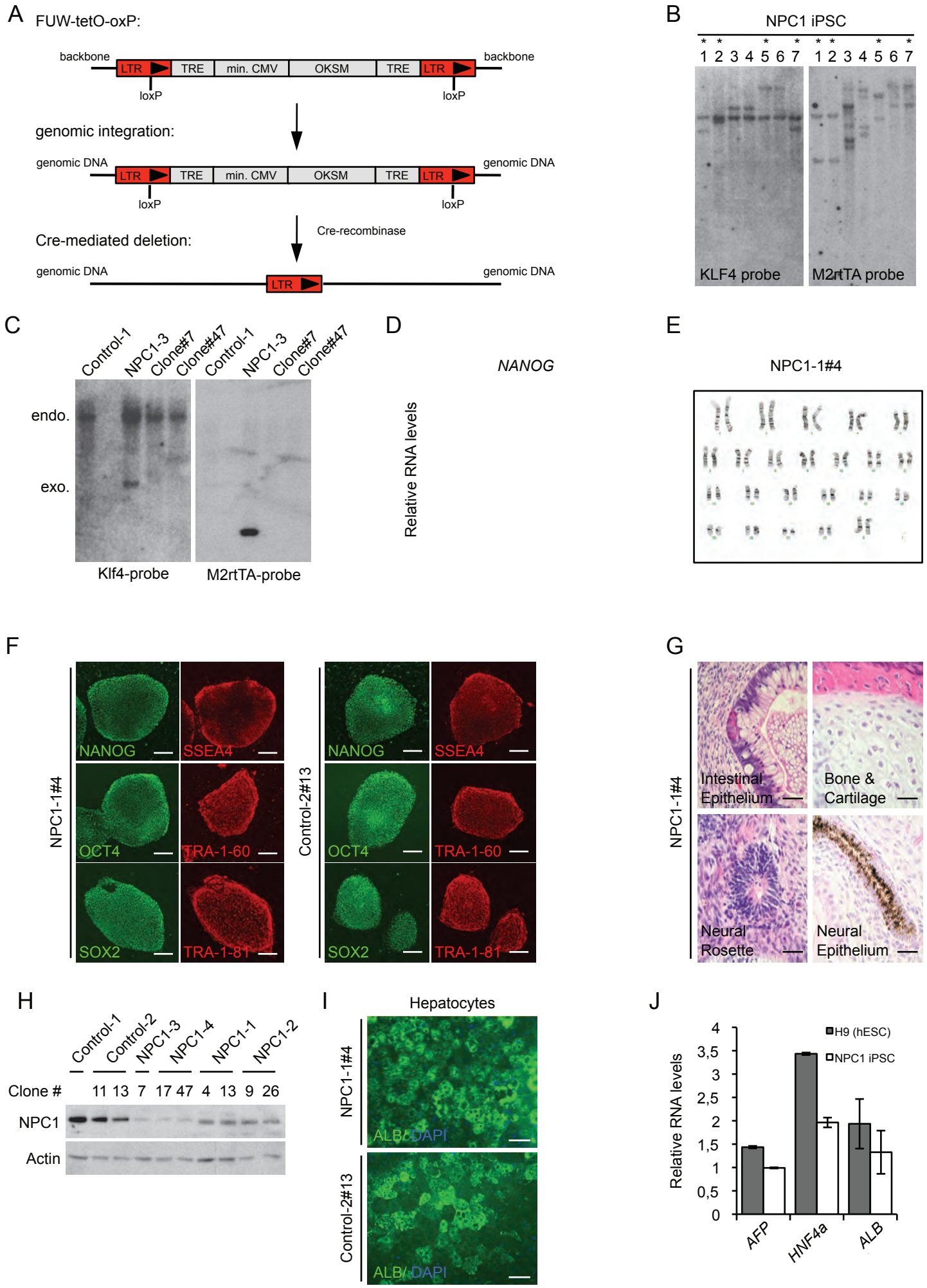
A
FUW-tetO-oxP:
backbone
LTR
TRE
min. CMV
OKSM
TRE
LTR
backbone
loxP
loxP
genomic integration:
genomic DNA
genomic DNA
Cre-mediated deletion:
Cre-recombinase
B
NPC1 iPSC
1 2 3 4 5 6 7 1 2 3 4 5 6 7
KLF4 probe
M2rtTA probe
C
Control-1
NPC1-3
Clone#7
Clone#47
endo.
exo.
Klf4-probe
M2rtTA-probe
D
NANOG
Relative RNA levels
E
NPC1-1#4
F
NPC1-1#4
Control-2#13
NANOG
SSEA4
OCT4
TRA-1-60
SOX2
TRA-1-81
G
NPC1-1#4
Intestinal Epithelium
Bone & Cartilage
Neural Rosette
Neural Epithelium
H
Control-1
Control-2
NPC1-3
NPC1-4
NPC1-1
NPC1-2
Clone # 11 13 7 17 47 4 13 9 26
NPC1
Actin
I
Hepatocytes
NPC1-1#4
Control-2#13
ALB/ DAPI
J
H9 (hESC)
NPC1 iPSC
Relative RNA levels
4
3,5
3
2,5
2
1,5
1
0,5
0
AFP
HNF4a
ALB

Figure S2

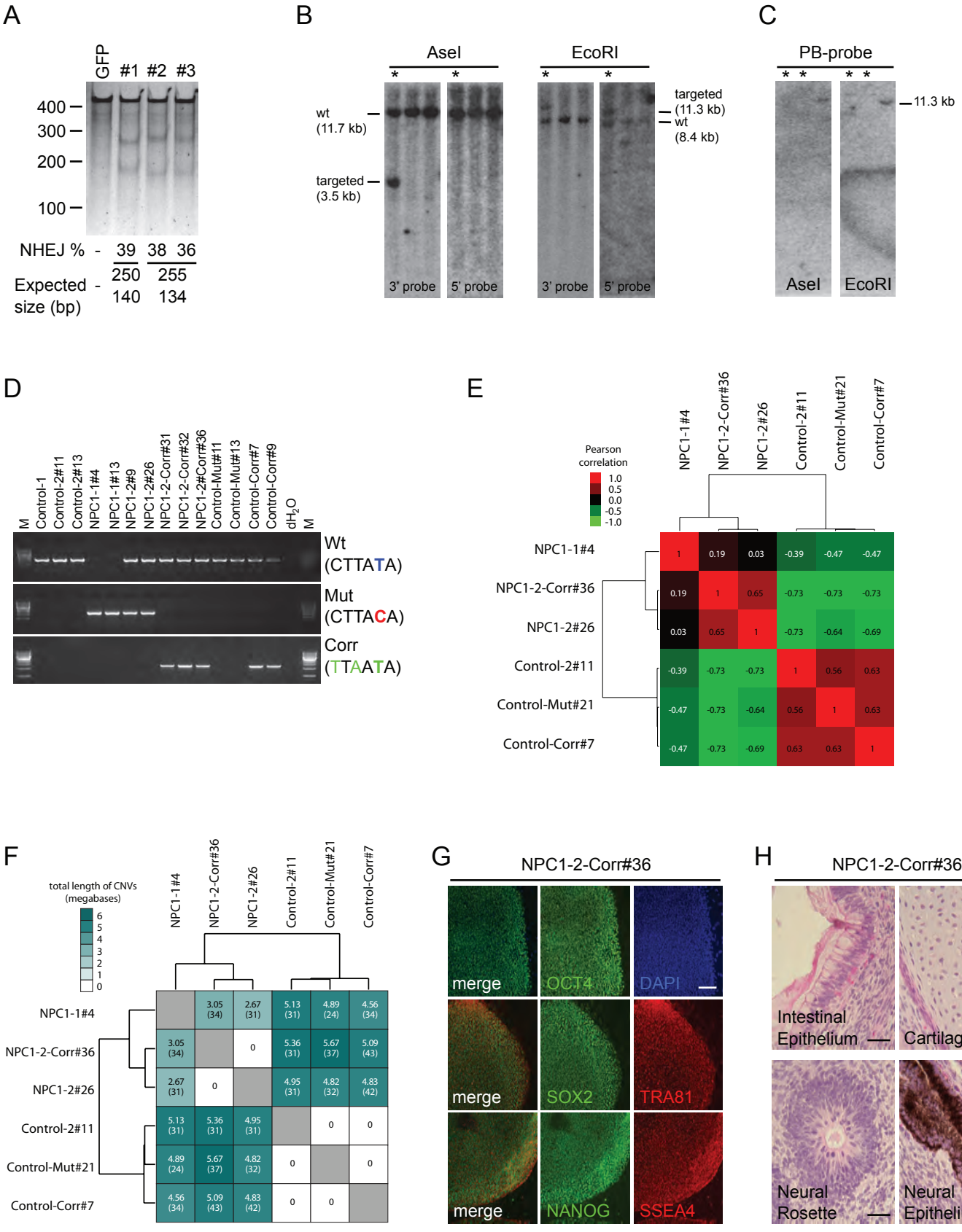
A
GFP
#1
#2
#3
400
300
200
100
NHEJ % - 39 38 36
Expected - 250 255
size (bp) 140 134
B
AseI
EcoRI
wt
(11.7 kb)
targeted
(3.5 kb)
targeted
(11.3 kb)
wt
(8.4 kb)
3' probe
5' probe
3' probe
5' probe
C
PB-probe
11.3 kb
AseI
EcoRI
D
M
Control-1
Control-2#11
Control-2#13
NPC1-1#4
NPC1-1#13
NPC1-2#9
NPC1-2#26
NPC1-2-Corr#31
NPC1-2-Corr#32
NPC1-2#Corr#36
Control-Mut#11
Control-Mut#13
Control-Corr#7
Control-Corr#9
dH2O
M
Wt
(CTTATA)
Mut
(CTTACA)
Corr
(TTAATA)
E
Pearson
correlation
1.0
0.5
0.0
-0.5
-1.0
NPC1-1#4
NPC1-2-Corr#36
NPC1-2#26
Control-2#11
Control-Mut#21
Control-Corr#7
F
total length of CNVs
(megabases)
6
5
4
3
2
1
0
G
NPC1-2-Corr#36
merge
OCT4
DAPI
merge
SOX2
TRA81
merge
NANOG
SSEA4
H
NPC1-2-Corr#36
Intestinal
Epithelium
Cartilage
Neural
Rosette
Neural
Epithelium

Figure S3

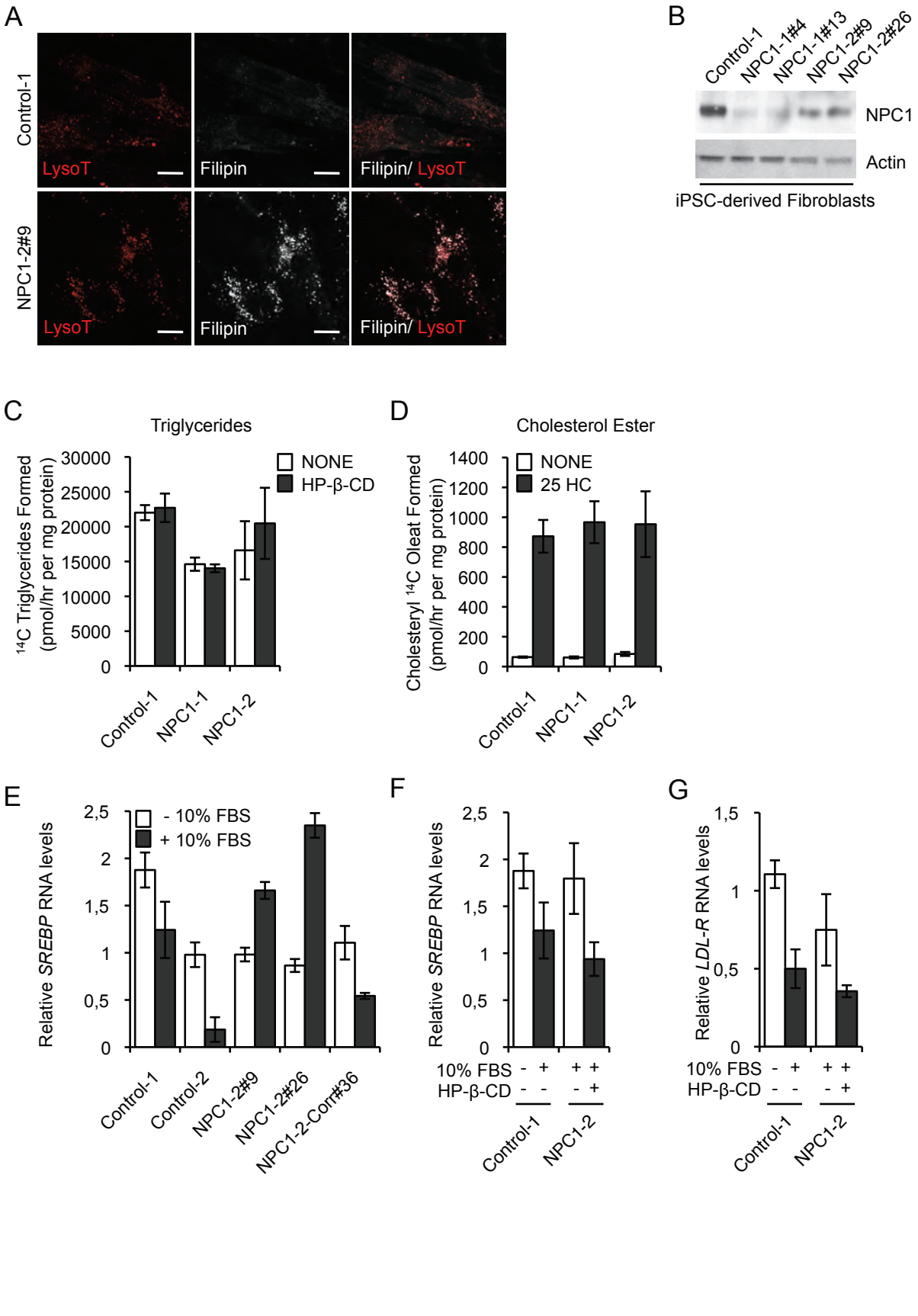
A
Control-1
NPC1-2#9
LysoT
Filipin
Filipin/ LysoT
B
Control-1
NPC1-1#4
NPC1-1#13
NPC1-2#9
NPC1-2#26
NPC1
Actin
iPSC-derived Fibroblasts
C
Triglycerides
14C Triglycerides Formed (pmol/hr per mg protein)
NONE
HP-β-CD
Control-1
NPC1-1
NPC1-2
D
Cholesterol Ester
Cholesteryl 14C Oleat Formed (pmol/hr per mg protein)
NONE
25 HC
E
Relative SREBP RNA levels
- 10% FBS
+ 10% FBS
Control-1
Control-2
NPC1-2#9
NPC1-2#26
NPC1-2-Corr#36
F
Relative SREBP RNA levels
10% FBS
HP-β-CD
G
Relative LDL-R RNA levels

Figure S4

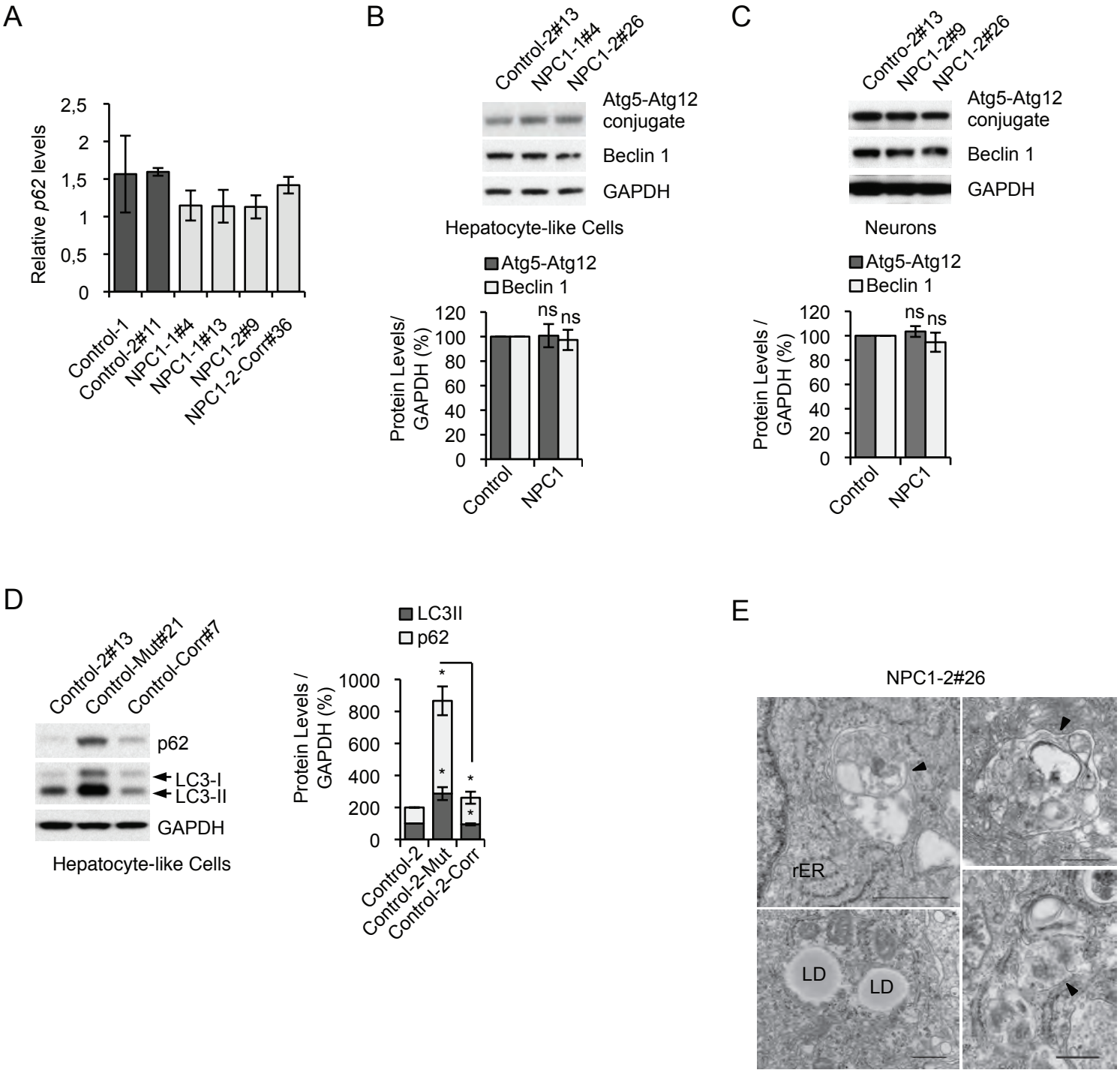
A
Relative p62 levels
2,5
2
1,5
1
0,5
0
Control-1
Control-2#11
NPC1-1#4
NPC1-1#13
NPC1-2#9
NPC1-2-Corr#36
B
Control-2#13
NPC1-1#4
NPC1-2#26
Atg5-Atg12 conjugate
Beclin 1
GAPDH
Hepatocyte-like Cells
Atg5-Atg12
Beclin 1
Protein Levels/ GAPDH (%)
120
100
80
60
40
20
0
ns
ns
Control
NPC1
C
Contro-2#13
NPC1-2#9
NPC1-2#26
Atg5-Atg12 conjugate
Beclin 1
GAPDH
Neurons
Atg5-Atg12
Beclin 1
Protein Levels / GAPDH (%)
120
100
80
60
40
20
0
ns
ns
Control
NPC1
D
Control-2#13
Control-Mut#21
Control-Corr#7
p62
LC3-I
LC3-II
GAPDH
Hepatocyte-like Cells
LC3II
p62
Protein Levels / GAPDH (%)
1000
800
600
400
200
0
*
*
*
*
Control-2
Control-2-Mut
Control-2-Corr
E
NPC1-2#26
rER
LD
LD

Figure S5

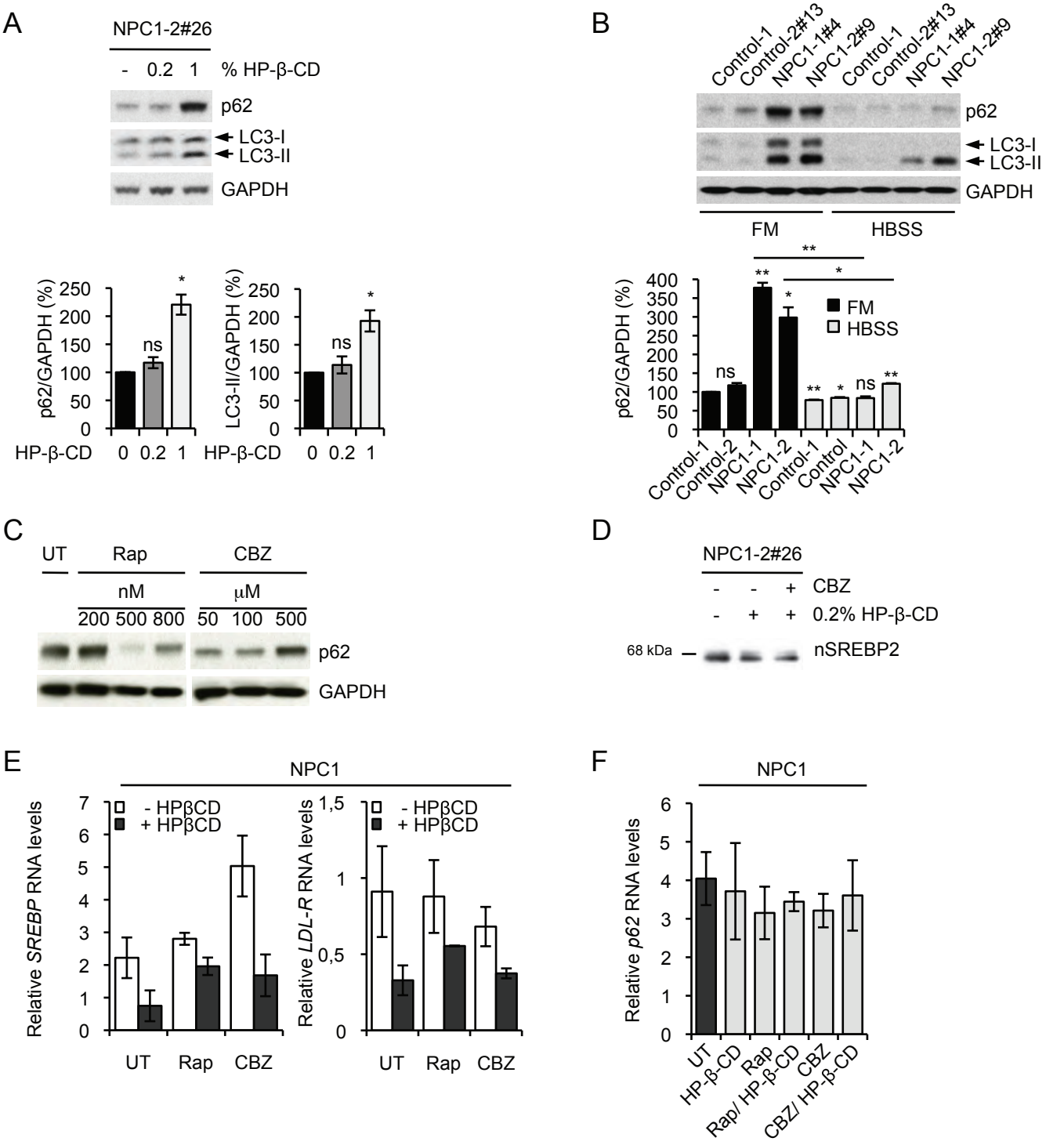

G

Table: Effect of Autophagy Inducers used in Hepatic and Neuronal Cultures

Autophagy Inducer	Mechanism of Action	Concentration	Effective in: Hepatic-like cultures	Neuronal cultures
Rapamycin (Rap)	mTORCI Inhibitor	500 nM	Yes	Yes
Carbamazepine (CBZ)	Inositol and IP_3 reducing agent	100 μM	Yes	Yes
Verapamil (Ver)	Ca^{2+} channel blocker	5 μM	No	Yes
Trehalose (Tre)	unknown	10 nM	No	Yes
SMER28	unknown	100 μM	No	n/a

Table S1: Summary of TALEN-mediated Genome Editing

Cell Line	TALEN Pair/ Donor Vector	Number of Clones Analyzed	Number of Clones with Modified Tareget Locus	Number of Clones Treated with Transposaes	Number of Correctly Targeted/ Analyzed Clones	Number of Off-Target Modifications/ Tested Sites	Clone ID	Cell Line
WIBR-IPS-NPC1$^{1920delG/wt}$	12/ PB	117	4 (2 wt allele)	2	2 / 81	0 / 10	control-Corr (#7, #9)	WIBR-IPS-NPC1$^{1920delG/corr}$
WIBR-IPS-NPC1$^{P237S/\ I1061T}$	12/ PB	146	5 (4 I1062T allele)	5	2 / 287	0 / 10	NPC1-2-Corr (#32, #36)	WIBR-IPS-NPC1$^{P237S/\ I1062T-Corr}$

Supplemental Figures and Tables

Figure S1: Generation and Characterization of NPC Patient-Specific iPSCs, Related to Figure 1

(A) Schematic overview depicting the reprogramming strategy used to generate factor-free NPC patient-specific iPSCs using the FUW-tetO-loxP polycystronic vector.

(B) Southern blot analysis showing number of integrations of FUW-tetO-losxP and M2rtTA-loxP respectively in derived NPC1 iPSCs. Genomic DNA was digested with BamHI and hybridized with an internal Klf4 and M2rtTA-probe respectively. Lanes 1 to 7 contain different NPC1 iPSC clones of one representative fibroblast line. Clones with the lowest number of integrations are marked with an asterisk.

(C) Southern blot analysis showing derived NPC1 iPSCs before and after Cre-mediated excision of FUW-tetO-losxP and M2rtTA-loxP. Genomic DNA was digested with HindIII and hybridized with an internal Klf4- and M2rtTA-probe respectively. Fragment sizes for each digest are indicated.

(D) Quantitative RT-PCR assay for expression analyses of endogenous pluripotency marker, *NANOG*. Data shown are relative to *GAPDH*. Graphical data represent mean ± SD (n = 2) of independent experiments.

(E) Karyotype analysis of a representative NPC1 iPSC line.

(F) Immunofluorescence staining for pluripotency markers NANOG, OCT4, SOX2, SSEA4, TRA-1-60 and TRA-1-81 in one representative NPC1 iPSCs and Control-2 line (scale bar 200 μm).

(G) Hematoxylin and eosin staining of teratoma section generated from a representative NPC1 iPSC line (scale bar 50 μm).

(H) Immunoblot analysis in NPC1 iPSC and Control lines with NPC1 and Actin antibodies detecting NPC1 protein levels in indicted clones.

(I) Immunofluorescence staining of hepatocyte-like cultures derived from a representative NPC1 iPSC and Control-2 iPSC line 21 days after induction of hepatocyte differentiation for human Albumin (ALB; green). Nuclei are stained with DAPI (blue) (scale bar 100 μm).

(J) Quantitative RT-PCR expression analyses of hepatocyte-specific markers, such as α-fetoprotein (AFP), HNF4α and Albumin (ALB), 21 days after induction of differentiation. Data shown are relative to *GAPDH*. Graphical data represent mean ± SD (n = 2) of independent experiments.

Figure S2: Correction of *NPC1*^{I1061T} Mutation in Patient-Specific iPSCs, Related to Figure 2

(A) Assay of TALEN activity with the Surveyor nuclease. The *NPC1* locus was amplified and modification of the locus was measured using the Surveyor nuclease. The expected sizes of correctly digested fragments are indicated. Cleavage efficiency was quantified and shown below each lane. GFP indicates GFP control transfection.

(B) Southern blot analysis of NPC1-2 line targeted with PB donor plasmid PB-NPC1-I1061T. Genomic DNA was digested with indicated enzymes and hybridized with the external 3' and 5' probe. Fragment sizes of wild type (wt) and targeted alleles for each digest are indicated. Correctly targeted clones are marked with an asterisk.

(C) Southern blot analysis of NPC1 iPSCs targeted with PB donor plasmid PB-*NPC1*^{I1061T} after excision of PB-TR flanked selection cassette. Genomic DNA was digested with indicated enzymes and hybridized with a PB-probe. Fragment size of

targeted allele is indicated. Clones showing no residual PB integration are marked with an asterisk.

(D) PCR of indicated cell lines was performed with specific primers detecting wild type (wt, upper lane), mutant (Mut, middle lane) and corrected (Corr, lower lane) sequence in *NPC1* locus.

(E) Genome wide copy number variation (CNV) analysis showing the correlation of indicated NPC1 iPSC lines and their isogenic counterparts. Values indicate the Pearson correlation coefficient between copy number profiles. Allosomes were excluded.

(F) Matrix showing the total length of CNVs (in mega bases, including gain and loss) identified in each pair-wise comparison, with the number of CNV regions in parentheses. Minimum CNV width was defined as 30kb and allosomes were excluded.

(G) Immunofluorescence for pluripotency markers, such as OCT4, SOX2, Tra-1-81, NANOG and SSEA4, in one representative NPC1-2-Corr clone (scale bar 100 μm).

(H) Hematoxylin and eosin staining of teratoma sections from one representative NPC1-2-Corr clone (scale bar 50 μm).

Figure S3: Analysis of Cholesterol Metabolism in isogenic NPC1 iPSC-Derived Cells, Related to Figure 3

(A) LysoTracker and Filipin staining in representative Control-2 and NPC1 iPSC derived fibroblast lines. Results shown are representative of two independent experiments. Scale bar 10 μm.

(B) Immunoblot analysis showing NPC1 and Actin protein levels in fibroblasts derived from indicted NPC1 iPSC lines. Data shown are representative for two independent experiments.

(C) Triglycerides synthesis in hepatic cultures derived from indicated Control and NPC1 iPSC lines after HP-ß-Cyclodextrin (HP-ß-CD) treatment. Mean variation for each of the duplicate incubations for Control-1, NPC1-1 and NPC1-2 were in a range between 0.1 and 39% respectively.

(D) Cholesteryl ester formation in hepatic cultures derived from indicated Control and NPC1 iPSC lines after treatment with 25-hydroxycholesterol (25-HC). Mean variation for each of the duplicate incubations for Control-1, NPC1-1 and NPC1-2 were a range between 2 and 14% respectively.

(E) Quantitative RT-PCR assay for expression analyses of *SREBP* RNA levels in NPC1 iPSC-derived hepatic cultures of control (Control-1, Control-2), NPC1-deficient (NPC1-1, NPC1-2) and corrected (NPC1-2-Corr) before (-) and after (+) exposure to 10% FBS. Data shown are relative to *GAPDH*. Graphical data represent mean ± SD (n = 3).

(F) Quantitative RT-PCR assay for expression analyses of *SREBP* RNA levels in NPC1 iPSC-derived hepatic cultures comparing Control-1 after exposure to 10% FBS and NPC1-2 line after 0.2% HP-ß-CD treatment as indicated below the graph. Data shown are relative to *GAPDH*. Graphical data represent mean ± SD (n = 3).

(G) Quantitative RT-PCR assay for expression analyses of *LDL-R* RNA levels in NPC1 iPSC-derived hepatic cultures comparing Control-1 line after exposure to 10% FBS and NPC1-2 line after exposure to 10% FBS and 0.2% HP-ß-CD treatment as indicated. Data shown are relative to *GAPDH*. Graphical data represent mean ± SD (n = 3).

(E-G) Results shown are representative for at three independent experiments.

Figure S4: Genetic Correction of Autophagy Phenotype in NPC1 iPSC-derived cells, Related to Figure 4

(A) Quantitative RT-PCR expression analyses of *p62* RNA levels in Control-1 and NPC1 iPSC-derived hepatic cultures. Data shown are relative to *GAPDH*. Graphical data represent mean ± SD (n = 2).

(B, C) Immunoblot analysis and quantification of Beclin-1 and Atg5-Atg12 conjugation levels using anti-Beclin-1, anti-Atg5 and anti-GAPDH antibodies in Control and NPC1 iPSC-derived hepatic (B) and neuronal cultures (C). Graphical data represent mean ± SE (n = 3). *p* values of Beclin-1 levels compared to Control sample: 0.7731 (NPC1) (B); 0.1863 (NPC1) (C). *p* values of Atg5-Atg12 conjugation levels compared to Control sample:0.9432 (NPC1) (B); 0.3897 (C).

(D) Immunoblot analysis and quantification of p62 and LC3-II levels in hepatic cultures derived from Control-2 after disruption and repair of the *NPC1* wt allele using specific antibodies. *p* values compared to Control sample: 0.0333 (p62, Control-2-Mut), 0.2195 (p62, Control-2-Corr); 0.0435 (LC3-II, Control-2-Mut), 0.4756 (LC3-II, Control-2-Corr). *p* values compared to Control-2-Mut sample: 0.0299 (p62, Control-2-Corr), 0.0383 (LC3-II, Control-2-Corr).

(A-D) Results shown are representative of at least two independent experiments using different clones of each line. ***, $p < 0.001$; **, $p < 0.01$; *, $p < 0.05$; ns, non-significant.

(E) Representative electron microscopy images of autophagic vacuoles assessed in NPC1 iPSC-derived hepatic-like cells. Lipid droplets (LD), rough endoplasmatic reticulum (rER) are indicated. Scale bar, 500 nm.

Figure S5: Chemical Correction of Autophagy Phenotype in NPC1 iPSC-derived cells, Related to Figure 5

(A) Immunoblot analysis and quantification of p62 and LC3-II levels using anti-p62, anti-LC3 and anti-GAPDH antibodies in NPC1 iPSC-derived hepatic cultures, either left untreated or treated with indicated concentrations of HP-ß-Cyclodextrin (HP-ß-CD) over 5 days. Graphical data represent mean ± SE (n = 3). *p* values of p62 levels compared to untreated sample: 0.2233 (0.2% HP-ß-CD); 0.0213 (1% HP-ß-CD). *p* values of LC3-II levels compared to untreated sample: 0.4614 (0.2% HP-ß-CD); 0.0395 (1% HP-ß-CD).

(B) Immunoblot analysis and quantification of p62 levels using anti-p62 and anti-GAPDH antibodies in Control and NPC1 iPSC-derived hepatic cultures, cultured either in basal (full medium; FM) or starvation (HBSS) condition. Graphical data represent mean ± SE (n = 3). *p* values of p62 levels compared to Control-1 FM sample: 0.1033 (Control-2 FM); 0.0023 (NPC1-1 FM); 0.0184 (NPC1-2 FM); 0.0036 (Control-1 HBSS); 0.0155 (Control-2 HBSS); 0.0699 (NPC1-1 HBSS); 0.0055 (NPC1-2 HBSS). *p* values of p62 levels compared to NPC1-1 FM sample: 0.0023 (NPC1-1 HBSS). *p* values of p62 levels compared to NPC1-2 FM sample: 0.0232 (NPC1-2 HBSS).

(C) Immunoblot analysis of p62 levels using anti-p62 and anti-GAPDH antibodies in NPC1 iPSC-derived hepatic cultures using indicated concentrations of rapamycin (Rap) and carbamazepine (CBZ). Note that CBZ-treated section (right) is part of the same immunoblot (on the left), where the intermediate lanes have been excised for simplifying representation.

(D) Immunoblot of nuclear sterol regulatory element-binding protein 2 (SREBP2) in NPC1-2 hepatic cells after incubation with 10% FBS and treatment with 0.2% HP-β-Cyclodextrin (HP-β-CD) alone or in combination with CBZ. Protein sizes are indicated.

(E) Quantitative RT-PCR expression analyses of *SREBP* and low density lipoprotein receptor (*LDL-R*) RNA levels in NPC1 iPSC-derived hepatic cultures after treatment with 0.2% HP-β-CD alone or in combination with Rap or (CBZ). Data is shown are relative to *GAPDH*. Graphical data represent mean ± SD (n = 3).

(F) Quantitative RT-PCR expression analyses of *p62* RNA levels in Control and NPC1 iPSC-derived hepatic cultures. Data shown are relative to *GAPDH*. Graphical data represent mean ± SD (n = 3).

(G) Table: Effect of autophagy inducers used in hepatic-like and neuronal cultures with working concentration indicated.

Results shown are representative of at least three independent experiments using different clones of each line. ***, $p < 0.001$; **, $p < 0.01$; *, $p < 0.05$; ns, non-significant.

Table S1: Summary of TALEN-mediated Genome Editing, Related to Figure 2

Supplemental Methods

Cell culture

HESCs WIBR3 (Whitehead Institute Center for Human Stem Cell Research, Cambridge, MA) (Lengner et al., 2010) and hiPSCs were cultivated as described previously (Hockemeyer et al., 2008; Soldner et al., 2009). Briefly, hiPSCs and hESCs were maintained on mitomycin C inactivated mouse embryonic fibroblast (MEF) feeder layers in hESC medium [DMEM/F12 (Invitrogen) supplemented with 15% fetal bovine serum (FBS) (Hyclone), 5% KnockOut Serum Replacement (Invitrogen), 1 mM glutamine (Invitrogen), 1% nonessential amino acids (Invitrogen), 0.1 mM ß-mercaptoethanol (Sigma) and 4 ng/ml FGF2 (R&D Systems)]. Cultures were passaged every 5 to 7 days either manually or enzymatically with collagenase type IV (Invitrogen; 1.5 mg/ml). Differentiation into hepatic-like cells and neurons was induced as described previously (Si-Tayeb et al., 2010). Briefly, hiPSCs were plated on matrigel coated plates as single cells and cultured in ROCK inhibitor 24 hr. After reaching 80% confluence differentiation was initiated following published protocols. As described previously neuro progeniors (NPs) and neurons were derived using an embryoid body (EB) based protocol (Marchetto et al., 2010).

Lentiviral Infection and derivation of transgene-free hiPSC

Transgene-free hiPSCs were generated as described previously (Soldner et al., 2009; Takahashi et al., 2007). Briefly, VSV-G pseudotyped lentiviruses encoding a cre-excisable and doxycycline-inducible polycistronic Oct4, Klf4, Sox2 and c-Myc expression cassette (pHAGE2-tetOminiCMV-hSTEMCCA) (Sommer and Mostoslavsky,

2010) or a constitutive reverse tetracycline transactivator flanked by loxP sides (FUW-M2rtTA) (Hockemeyer et al., 2008) were generated in 293T cells(Brambrink et al., 2008). Four consecutive infections of NPC1 patient fibroblasts were performed over a period of 48 hr. Patient fibroblasts lines (Coriell Institute for Medical Research) were passaged and re-plated five days after transduction. Reprogramming was induced 48 hr after plating using hESC medium containing doxycycline (Sigma-Aldrich; 2 mg/ml). HiPSC colonies were picked between 3 and 5 weeks after doxycycline-induction and maintained in the absence of doxycycline. Individual clones were analyzed by Southern blot. Genomic DNA was separated on a 0.7% agarose gel after restriction digest with EcoRI, transferred to a nylon membrane (Amersham) and hybridized with ^{32}P random primer (Stratagene) labeled probes against hKLF4 (full length hKLF4 cDNA), and M2rtTA (full length M2rtTA cDNA). hiPSC clones with the lowest number of integrations were chosen for transgene excision. hiPSC lines were cultured in ROCK inhibitor (Stemgent) 24 hr prior to electroporation. Cells were harvested using 0.05% trypsin/EDTA solution (Invitrogen), resuspended in PBS and co-transfected with pTurbo-Cre (40 mg; GenBank Accession Number AF334827) and pEGFP-N1 (10 mg; Clontech) by electroporation (Gene Pulser Xcell System, Bio-Rad: 250 V, 500 mF, 0.4 cm cuvettes). Excision of the reprogramming transgenes and the M2rtTA transactivator was confirmed by southern blot as described above using HindIII digestion.

Teratoma Formation and Karyotype Analysis

HiPSCs were collected and resuspended in 150 µl of PBS. Cells were injected subcutaneously in the back of SCID mice (two mice per cell line, Taconic). After 4 to 8 weeks mice were euthanized, tumors were isolated and fixed in formalin. Samples were

paraffin imbedded, sectioned and analyzed based on hematoxylin and eosin staining. Karyotype analysis of generated hiPSCs was performed by Cell Line Genetics (Madison, WI).

Immunostaining

Immunostaining was performed according to standard protocols using the following primary antibodies: hSOX2 (goat polyclonal, R&D Systems); Oct-3/4 (mouse monoclonal, Santa Cruz Biotechnology); hNANOG (Cat. No. AF1997, goat polyclonal, R&D Systems); SSEA4 (mouse monoclonal, Developmental Studies Hybridoma Bank); Tra-1-60, (mouse monoclonal, Chemicon International); Tra-1-60, (Cat. No. MAB4360, mouse monoclonal, Millipore); AFP (Cat. No. A8452, mouse monoclonal, Sigma), HNF4a (goat polyclonal, Santa Cruz), hAlb (Cat. No. CL2513A, mouse monoclonal, Cedarlane), TuJ1 (mouse monoclonal, Covance); MAP2 (rabbit polyclonal, Sigma); Nestin (Cat. No. AB5922, mouse monoclonal, Milipore), Pax6 (Cat. No. PRB-278P, rabbit polyclonal, Covance); appropriate Alexa Fluor dye conjugated secondary antibodies (Invitrogen) were used. Visualization of lysosomes in fixed cells was performed using LysoTracker Red DND-99 according to the manufacturer protocol (Life Technologies). Slides were mounted with Fluoromount G (Emsdiasum) and analyzed (LSM710, Zeiss; Eclipse Ti - Nikon). Images were taken using LSM710 confocal microscope (Zeiss) or inverted microscope (Eclipse Ti - Nikon).

Apoptosis assay

FITC-Annexin V and Propidium Iodine staining were performed according to manufacturer instructions (BD Bisciences). Cells were analyzed using LSR FACS.

Detection and quantification of apoptotic cells in neuronal cultures was preformed by counting fragmented nuclei and based on labeling of DNA strand breaks (TUNEL technology) according to manufacturer instructions (*In situ* Cell Death Detection Kit, Roche).

RT-PCR

Total RNA of cells was prepared according to the manufacturer's instructions (Qiagen) and DNase-treated (R&D). A total of 300 ng of total RNA was reverse transcribed. Control PCRs were performed using *Gapdh* primers. Products were separated on a 2% agarose gel. PCR primers used were published previously (Funakoshi et al., 2011; Soldner et al., 2009). For quantitative PCR, reactions were performed with SYBR Green dye (Applied Biosystems). Results were analyzed using the delta-delta Ct method with *Gapdh* as a normalization control. Error bars are indicating s.d. of biological triplicates.

Immunoblot analysis

Cell pellets were lysed on ice in Lysis Buffer (10 mM Tris-HCl pH 7.4, 2% sodium dodecyl sulphate, 1 mM DTT, 10% glycerol, and 120 mg/ml urea) for 30 min in presence of Complete EDTA-free Protease Inhibitor Cocktail (Roche Diagnostics), boiled for 10 min at 95ºC and subjected to SDS-PAGE and immunoblot analysis. Blots were blocked with 10% non-fat milk powder in PBS-Tween 20 for 1 h at RT. Primary antibodies used were mouse NPC1 (Cat. No. AT3083a, mouse, monoclonal; ABGENT), Actin (Cat. No. sc-1616, goat, polyclonal; Santa Cruz), SREBP2 (1D2, mouse, monoclonal, J.L. Goldstein & M.S. Brown Lab), p62 (Cat. No 610832, mouse,

monoclonal; BD Bioscience), LC3 (Cat. No. NB100-2220, rabbit, polyclonal; Novus Biologicals), GAPDH (Cat. No. sc-47724, mouse, monoclonal; Santa Cruz), Atg5/Atg12 protein complex (Cat. No. 0262-100/ATG5-7C6, mouse, monoclonal, Nanotools), and Beclin 1 (Cat. No. 3738, rabbit, polyclonal; Cell Signaling Technology) respectively in concentrations as recommended. Blots were incubated with primary antibodies overnight at 4°C or 1 h at RT. Subsequently immunoblots were probed with anti-mouse, anti-rabbit, and anti-guinea pig IgG-HRP (H+L) secondary antibody respectively (1:5,000 dilutions, Cat. No. 401253, Cat. No. 401393, all EMD Biosciences) for 1 h at room temperature, and visualized using Amersham ECL Western Blotting Detection Reagent (GE Healthcare).

NPC1 TALENs Recognition Sequences and Prediction of off-target sites

The position weight matrices (PWMs) of NPC1 TALENs (NPC1Left and NPC1Right) were constructed using model 3 as described (Moscou and Bogdanove, 2009) with a pseudo-weight of 0.99 for observed di-residues. A PWM $\{P_{ij}\}$ of width w (where i is a position from 1 to w and j is a nucleotide from {A,C,G,T}) was converted into a position score matrix (PSM) $S_{ij}=10^3\log_2(P_{ij})$. The score of a potential binding site is defined as the sum of the scores of each position of the binding site against the PSM. A relative score was then calculated by subtracting the score of the site by the score of the consensus sequence. The relative score represents the relative affinity (in $\log_2$) for binding to that site compared to a site with the consensus sequence. All NPC1Left binding sites (hits) with a minimum relative score of -16,610 (corresponding to $\sim 10^5$ weaker predicted binding affinity) were found in the human genome (hg18). Binding sites of NPC1Right with minimum relative score of -16,610 were found with a spacer of

11-26 bp from each NPC1Left hit. The total relative score of a paired hit is defined as the sum of the NPC1Left and the NPC1Right relative scores and was used to rank the predicted target sites.

Table S2: TALEN Recognition Sequences and the Amino Acid Identity of the Repeat Variable Di-residues (RVDs) in the Corresponding TALENs

TALEN	TALEN recognition sequences (bold and underlined) & Amino acid sequence of the RVDs
***NPC1* pair 1**	5' **CTGAAGAAAGCCCGACT**TACAGCCAGTAATGTCACCGAAACCATGGGCATT 3'GACTTCTTTCGGGCTGAAT**G**TCGGTCATTACAG**TGGCTTTGGTACCCGTAA** HD NG NN NI NI NN NI NI NI NN HD HD HD NN NI HD NG (left TALEN) NI NI NG NN HD HD HD NI NG NN NN NG NG NG HD NN NN NG (right TALEN)
***NPC1* pair 2**	5'**GACGCTCTGAAGAAAGCCC**GACTTATAGCCAGTAATGTCACCGAAACCATG GGC 3' CTGCGAGACTTCTTTCGGGCTGAATATCGGTCAT**TACAGTGGCTTTGGTACCC G** NN NI HD NN HD NG HD NG NN NI NI NN NI NI NI NN HD HD HD (left TALEN) NN HD HD HD NI NG NN NN NG NG NG HD NN NN NG NN NI HD NI NG (right TALEN)
***NPC1* pair 3**	5'**GACGCTCTGAAGAAAGCC**GACTTATAGCCAGTAATGTCACCGAAACCATGG GC 3'CTGCGAGACTTCTTTCGGGCTGAATATCGGTCA**TTACAGTGGCTTTGGTACC CG** NN NI HD NN HD NG HD NG NN NI NI NN NI NI NI NN HD HD (left TALEN) NN HD HD HD NI NG NN NN NG NG NG HD NN NN NG NN NI HD NI NG NG (right TALEN)

Table S3: Predicted TALEN off Target Cutting Sides

Location	Spacer Length	Pair 1 match (%)	Pair 2 match (%)	Combined Score
chr2	23	CcaAAGAAAaCCCcACa (70.59)	AAaaCCCAaGaTTTCGtT (72.22)	-19360
chr7	12	CTcAAaAAAaCaaaACa (58.82)	AATGCCCATGaTTTCtcc (77.78)	-22165
chr3	18	aaGAAaAAAaCCCaAaa	AATaCCCATaaTTcCatT (66.67)	-22930
chrX	26	CTGAAGAActaCCaAaT (70.59)	AATGCCCcaGaTTTCcaT (72.22)	-23443
chr4	24	CaGcAGAcAaCCCaACT (70.59)	AcTGCCCATatTTTaatT (66.67)	-25144
chr10	24	CTGAAGAAcaaCCcACT (76.47)	AATcaCCATaaTTataaT (55.56)	-25180
chr1	17	CTGAAacAAaCCCcACa (70.59)	cATGCCtATaGTTcCaGc (66.67)	-25307
chr2	26	CTaAAcAAAcaCCaAaa (58.82)	AATGCCCATtGccTCaaT (72.22)	-25375
chr17	12	CTGAAaAAAaCCCcAac (70.59)	AAaaCaaATGGTTTCaca (61.11)	-25537
chr14	13	aTGAAGAAAGCCCaAta (76.47)	AATaCCaATatTTTaGaT (66.67)	-25648

Illumina sequencing and CNV analysis

Illumina whole-genome genotyping and copy number variation (CNV) analysis was performed using a standard protocol. 40-nt Illumina reads were mapped to the human genome with bowtie2 allowing 1 mismatch in the seed. After splitting the autosomes into 10kb windows (overlapping by 5kb), read coverage across each window was calculated and then scaled by the total number of mapped reads per sample. Counts were log-transformed, mean-centered by window, and Pearson correlation was calculated between

samples, which were then hierarchically clustered using average linkage. Mapped 40-nt Illumina reads were used to identify copy number variants (CNVs) throughout the autosomes using the CNV-seq package (http://www.ncbi.nlm.nih.gov/pubmed/19267900) from R. A CNV was defined relative to a two-sample comparison, with the minimum CNV width set as 30kb, and the total CNV width for each comparison was calculated. These total CNV widths were used to hierarchically cluster (with average linkage) the samples.

Electron microscopy analysis

Cells were fixed in 2.5% gluteraldehyde, 3% paraformaldehyde with 5% sucrose in 0.1 M sodium cacodylate buffer (pH 7.4), pelletted, and post-fixed in 1% OsO4 in veronal-acetate buffer. The cell pellet was stained in block overnight with 0.5% uranyl acetate in veronal-acetate buffer (pH 6.0), then dehydrated and embedded in Embed-812 resin. Sections were cut on a Reichert Ultracut E microtome with a Diatome diamond knife at thickness setting of 50 nm, stained with uranyl acetate and lead citrate. The sections were examined using a FEI Tecnai spirit at 80 KV and photographed with an AMT ccd camera. Analysis of the number of autophagic vacuoles (AVs) were performed on >30 electron micrographs per experimental sample as described previously (Yu et al., 2005).

Autophagy Inducing Chemical Compounds

To test the possibility of induce autophagy using small molecules we performed a candidate drug screen including described mTOR independent autophagy inducers (Sarkar, 2013).

Table S4: Small Molecule Autophagy Inducers and Tested Concentrations

Autophagy Inducer	Mechanism of Action	Concentration used In iPSC-derived Cultures	Induction of Autophagy
Rapamycin (Rap) (Blommaart et al., 1995)	mTORCI Inhibitor	200 nM*	No (hep/ neuro)
		400 nM	No (hep/ neuro)
		500 nM	Yes (hep/ neuro)
		800 nM	cell death
Carbamazepine (CBZ) (Sarkar et al., 2005)	Inositol and IP_3 reducing agent	50 μM*	Light (hep/ neuro)
		100 μM	Yes (hep/ neuro)
		500 μM	cell death
Verapamil (Ver) (Williams et al., 2008)	Ca^{2+} channel blocker	1 μM*	No (hep/ neuro)
		5 μM	only in neurons
		100 μM	cell death
Trehalose (Tre) (Sarkar et al., 2007a)	unknown	1 mM	No (hep/ neuro)
		10 mM	only in neurons
		100 mM*	No (hep/ neuro)
SMER28 (Sarkar et al., 2007b)	unknown	50 μM*	No (hep)/ n/a (neuro)
		100 μM	No (hep)/ n/a (neuro)
		500 μM	No (hep)/ n/a (neuro)

* Concentrations normally used in cell culture; n/a – not tested

Analysis of autophagosome synthesis by LC3-II levels using bafilomycin A_1

Autophagic flux involves the complete flow of the autophagosomes from their formation to fusion with lysosomes. Constitutive autophagy occurs in all mammalian cell types under basal conditions, where the synthesis of autophagosomes and autophagosomes–lysosome fusion occur at a normal rate. As the steady state levels of LC3-II are affected both by synthesis and degradation, effects on autophagy are assessed by clamping LC3-II/autophagosome degradation with a saturating concentration of bafilomycin A_1. Bafilomycin A_1 inhibits the vacuolar H^+ ATPase (V-ATPase) and prevents acidification of lysosomes, thereby inhibiting LC3-II degradation and subsequently blocks

autophagosomes–lysosome fusion, resulting in increased LC3-II levels compared to the basal (untreated) state (Klionsky et al., 2008) This is a well–established method for monitoring autophagosome synthesis (Yamamoto et al., 1998). Autophagosome synthesis was analyzed by measuring LC3-II levels relative to actin (loading control) in the presence of a saturating concentration of 400 nM bafilomycin A_1, treated for the last 6-8 h prior to harvesting the cells for immunoblot analysis (Klionsky et al., 2012; Klionsky et al., 2008; Rubinsztein et al., 2012). Cells were lysed and subjected to SDS–PAGE and immunoblot analysis with anti-LC3 antibody.

REFERENCES

Blommaart, E.F., Luiken, J.J., Blommaart, P.J., van Woerkom, G.M., and Meijer, A.J. (1995). Phosphorylation of ribosomal protein S6 is inhibitory for autophagy in isolated rat hepatocytes. J Biol Chem *270*, 2320-2326.

Brambrink, T., Foreman, R., Welstead, G.G., Lengner, C.J., Wernig, M., Suh, H., and Jaenisch, R. (2008). Sequential expression of pluripotency markers during direct reprogramming of mouse somatic cells. Cell Stem Cell *2*, 151-159.

Funakoshi, N., Duret, C., Pascussi, J.M., Blanc, P., Maurel, P., Daujat-Chavanieu, M., and Gerbal-Chaloin, S. (2011). Comparison of hepatic-like cell production from human embryonic stem cells and adult liver progenitor cells: CAR transduction activates a battery of detoxification genes. Stem Cell Rev *7*, 518-531.

Hockemeyer, D., Soldner, F., Cook, E.G., Gao, Q., Mitalipova, M., and Jaenisch, R. (2008). A drug-inducible system for direct reprogramming of human somatic cells to pluripotency. Cell Stem Cell *3*, 346-353.

Klionsky, D.J., Abdalla, F.C., Abeliovich, H., Abraham, R.T., Acevedo-Arozena, A., Adeli, K., Agholme, L., Agnello, M., Agostinis, P., Aguirre-Ghiso, J.A., *et al*. (2012). Guidelines for the use and interpretation of assays for monitoring autophagy. Autophagy *8*, 445-544.

Klionsky, D.J., Elazar, Z., Seglen, P.O., and Rubinsztein, D.C. (2008). Does bafilomycin A1 block the fusion of autophagosomes with lysosomes? Autophagy *4*, 849-950.

Lengner, C.J., Gimelbrant, A.A., Erwin, J.A., Cheng, A.W., Guenther, M.G., Welstead, G.G., Alagappan, R., Frampton, G.M., Xu, P., Muffat, J., *et al*. (2010). Derivation of pre-X inactivation human embryonic stem cells under physiological oxygen concentrations. Cell *141*, 872-883.

Marchetto, M.C., Carromeu, C., Acab, A., Yu, D., Yeo, G.W., Mu, Y., Chen, G., Gage, F.H., and Muotri, A.R. (2010). A model for neural development and treatment of Rett syndrome using human induced pluripotent stem cells. Cell *143*, 527-539.

Moscou, M.J., and Bogdanove, A.J. (2009). A simple cipher governs DNA recognition by TAL effectors. Science *326*, 1501.

Rubinsztein, D.C., Codogno, P., and Levine, B. (2012). Autophagy modulation as a potential therapeutic target for diverse diseases. Nat Rev Drug Discov *11*, 709-730.

Sarkar, S., Davies, J.E., Huang, Z., Tunnacliffe, A., and Rubinsztein, D.C. (2007a). Trehalose, a novel mTOR-independent autophagy enhancer, accelerates the clearance of mutant huntingtin and alpha-synuclein. J Biol Chem *282*, 5641-5652.

Sarkar, S., Floto, R.A., Berger, Z., Imarisio, S., Cordenier, A., Pasco, M., Cook, L.J., and Rubinsztein, D.C. (2005). Lithium induces autophagy by inhibiting inositol monophosphatase. J Cell Biol *170*, 1101-1111.

Sarkar, S., Perlstein, E.O., Imarisio, S., Pineau, S., Cordenier, A., Maglathlin, R.L., Webster, J.A., Lewis, T.A., O'Kane, C.J., Schreiber, S.L., *et al*. (2007b). Small molecules enhance autophagy and reduce toxicity in Huntington's disease models. Nat Chem Biol *3*, 331-338.

Si-Tayeb, K., Noto, F.K., Nagaoka, M., Li, J., Battle, M.A., Duris, C., North, P.E., Dalton, S., and Duncan, S.A. (2010). Highly efficient generation of human hepatocyte-like cells from induced pluripotent stem cells. Hepatology *51*, 297-305.

Soldner, F., Hockemeyer, D., Beard, C., Gao, Q., Bell, G.W., Cook, E.G., Hargus, G., Blak, A., Cooper, O., Mitalipova, M., *et al*. (2009). Parkinson's disease patient-derived induced pluripotent stem cells free of viral reprogramming factors. Cell *136*, 964-977.

Sommer, C.A., and Mostoslavsky, G. (2010). Experimental approaches for the generation of induced pluripotent stem cells. Stem Cell Res Ther *1*, 26.

Takahashi, K., Tanabe, K., Ohnuki, M., Narita, M., Ichisaka, T., Tomoda, K., and Yamanaka, S. (2007). Induction of pluripotent stem cells from adult human fibroblasts by defined factors. Cell *131*, 861-872.

Williams, A., Sarkar, S., Cuddon, P., Ttofi, E.K., Saiki, S., Siddiqi, F.H., Jahreiss, L., Fleming, A., Pask, D., Goldsmith, P., *et al*. (2008). Novel targets for Huntington's disease in an mTOR-independent autophagy pathway. Nat Chem Biol *4*, 295-305.

Yamamoto, A., Tagawa, Y., Yoshimori, T., Moriyama, Y., Masaki, R., and Tashiro, Y. (1998). Bafilomycin A1 prevents maturation of autophagic vacuoles by inhibiting fusion between autophagosomes and lysosomes in rat hepatoma cell line, H-4-II-E cells. Cell Struct Funct *23*, 33-42.

Yu, W.H., Cuervo, A.M., Kumar, A., Peterhoff, C.M., Schmidt, S.D., Lee, J.H., Mohan, P.S., Mercken, M., Farmery, M.R., Tjernberg, L.O., *et al.* (2005). Macroautophagy--a novel Beta-amyloid peptide-generating pathway activated in Alzheimer's disease. J Cell Biol *171*, 87-98.

Supplemental Note

Statistical Analyses (*p* values) of Main Figures

Figure 1: Generation and Characterization of Patient-Specific NPC1 iPSCs

(C) FACS analysis of cell viability and apoptosis in hepatic cultures. Graphical data (right panel) represent mean ± SE (n = 3). *p* values compared to Control-1: 0.0116 (NPC1-1); 0.0216 (NPC1-2), and Control-2; 0.0163 (NPC1-1); 0,0236 (NPC1-2).

(D) Analysis of cell death in TujI-positive neurons. Graphical data (right panel) represent ±SE (n = 3). *p* values compared to Control-1: 0.001 (NPC1-2#9); 0.0066, (NPC1-2#26), and Control-2#13: 0.0015 (NPC1-2#9); 0.0056 (NPC1-2#26).

Figure 4. Genetic Correction of Autophagy Phenotype in NPC1 iPSC-derived cells

(A) Quantification of p62 and LC3-II levels in hepatic cultures: Graphical data represent mean ± SE (n = 4). *p* values compared to Control-1: 0.0.0886 (LC3-II, Control-2), 0.0002 (LC3-II, NPC1-1), <0.0001 (LC3-II, NPC1-2); 0.0736 (p62, Control-2), <0.0001 (p62, NPC1-1), 0.002 (p62, NPC1-2).

(B) Quantification of p62 and LC3-II levels in neuronal cultures: Graphical data represent mean ± SE (n = 4). *p* values compared to Control-2: 0.0077 (LC3-II, NPC1-1), 0.0478 (LC3-II, NPC1-2); 0.0056 (p62, NPC1-1), 0.0212 (p62, NPC1-2).

(C) Quantification of LC3-II levels in hepatic cultures: Graphical data represent mean ± SE (n = 3). *p* values of LC3-II levels compared to Control-2 untreated (– $BafA_1$) sample: 0.0237 (NPC1-1 – $BafA_1$); 0.0356 (NPC1-2 – $BafA_1$). *p* values of LC3-II levels compared to Control-2 + $BafA_1$ sample: 0.12 (NPC1-1 + $BafA_1$); 0.1549 (NPC1-2 + $BafA_1$).

(D) Quantification of LC3-II levels in neuronal cultures: Graphical data represent mean ± SE (n = 3). *p* values of LC3-II levels compared to Control-2 untreated (– $BafA_1$) sample: 0.0488 (NPC1 – $BafA_1$). *p* values of LC3-II levels compared to Control-2 + $BafA_1$ sample: 0.0735 (NPC1 + $BafA_1$).

(E) Quantification of p62 and LC3-II levels in hepatic cultures: Graphical data represent mean ± SE (n = 3). *p* values compared to Control sample: 0.0269 (p62, NPC1-2), 0.8043 (p62, NPC1-2-Corr); 0.0457 (LC3-II, NPC1-2), 0.4712 (LC3-II, NPC1-2-Corr). *p* values compared to NPC1-2 sample: 0.0298 (p62, NPC1-2-Corr), 0.0439 (LC3-II, NPC1-2-Corr).

(F) Quantifications of p62 and LC3-II levels in neuronal cultures: Graphical data represent mean ± SE (n = 3). *p* values compared to Control sample: 0.0286 (p62, NPC1-2), 0.1449 (p62, NPC1-2-Corr); 0.0327 (LC3-II, NPC1-2), 0.4266 (LC3-II, NPC1-2-Corr). *p* values compared to NPC1-2 sample: 0.0107 (p62, NPC1-2-Corr), 0.0095 (LC3-II, NPC1-2-Corr).

(G) Quantification of autophagic vacuoles in electron microscopy images in hepatic-like cells. Graphical data represents mean ± SE (n = 3). *p* values compared to NPC1-2: 0.0169 (Control); 0.004 (NPC1-2-Corr).

Figure 5. Chemical Correction of Autophagy Phenotype in NPC1 iPSC-derived cells

(A) Quantification of p62 levels in hepatic cultures, treated with either DMSO (vehicle control) or rapamycin (Rap): Graphical data represent mean ± SE (n = 3). *p* values compared to Control-2 + DMSO sample: <0.0001 (Control-2 + Rap); 0.0003 (NPC1-1 + DMSO); 0.0489 (NPC1-1 + Rap); 0.0008 (NPC1-2 + DMSO); 0.0686 (NPC1-2 + Rap). *p* values compared to NPC1-1 + DMSO sample: 0.0007 (NPC1-1 + Rap). *p* values compared to NPC1-2 + DMSO sample: 0.0007 (NPC1-2 + Rap).

(B) Quantification of p62 levels in hepatic cultures after treatment with autophagy-inducing compounds: Graphical data represent mean ± SE (n = 3). *p* values compared to NPC1 UT sample: <0.0001 (Rap); <0.0001 (CBZ); 0.4522 (Ver); 0.8079 (Tre); 0.4156 (SMER28).

(C) Quantification of p62 levels in hepatic cultures, treated with CBZ and HP-ß-Cyclodextrin (HP-ß-CD) as indicated. Graphical data represent mean ± SE (n = 3). *p* values compared to NPC1 UT samples: 0.5628 (HP-ß-CD); 0.0002 (CBZ); 0.0065 (HP-ß-CD + CBZ). *p* values compared to NPC1 + HP-ß-CD sample: 0.0189 (HP-ß-CD + CBZ).

(E) Analysis of cell death in hepatic cultures after compound treatment. Graphical data represent mean ± SE (n = 3). *p* values compared to NPC1 UT samples: 0.0011 (Control UT); 0.5812 (HP-ß-CD); 0.0036 (Rap); 0.7494 (Rap + HP-ß-CD); 0.002 (CBZ); 0.0150 (CBZ + HP-ß-CD).

(F) Quantification of p62 levels neuronal cultures after treatment with autophagy-inducing compounds: Graphical data represent mean ± SE (n = 3). *p* values compared to NPC1 UT sample: 0.0156 (Rap); 0.0208 (CBZ); 0.0075 (Ver); 0.0204 (Tre).

(G) Analysis of cell death in neuronal cultures. Graphical data represent mean ± SE (n = 6). *p* values compared to NPC1-2#26 UT: <0.0001 (Control-2#13 UT); 0.004 (HP-ß-CD); < 0,0001 (Rap); < 0.0001 (Rap + HP-ß-CD); < 0.0001 (CBZ); < 0.0001 (CBZ + HP-ß-CD); 0.0002 (Tre); <0.0001 (Ver).